10680 *Inorg. Chem.* **2010**, *49*, 10680–10686
DOI: 10.1021/ic101708y

Inorganic Chemistry
Article

Formation of Diaryl Telluroxides and Tellurones by Photosensitized Oxygenation of Diaryl Tellurides

Makoto Oba,*,† Yasunori Okada,† Masaki Endo,† Kazuhito Tanaka,† Kozaburo Nishiyama,*,† Shigeru Shimada,‡ and Wataru Ando*,‡

†*Department of Materials Chemistry, Tokai University, Numazu, Shizuoka 410-0395, Japan, and*
‡*National Institute of Advanced Industrial Science and Technology (AIST), Tsukuba, Ibaraki 305-8565, Japan*

Received August 23, 2010

Aerobic oxygenation of diaryl tellurides under photosensitized conditions is investigated. Unlike Ph_2S and Ph_2Se, reaction of diaryl tellurides with singlet oxygen proceeds smoothly to yield diaryl telluroxides and the corresponding tellurones. The product distribution is largely affected by the substrate and the reaction conditions. In particular, the photooxygenation of bulky diaryl tellurides principally produces tellurones. The results of a series of trapping experiments suggest that the diaryl telluroxides can capture transient intermediates such as $Me_2S^+OO^-$ and $Ar_2Te^+OO^-$, generated in the singlet oxygen oxidation of chalcogenides, to yield diaryl tellurones, and therefore it may be the most potent precursors of the tellurones.

Introduction

Since the first report by Schenck and Krauch in 1962,[1] the reactions of diorganosulfides with singlet oxygen have been studied extensively[2] because of their relevance to the biological and antioxidation processes. Under standard photosensitized conditions, the oxidation of sulfides mainly produces sulfoxides, along with a small amount of sulfones. Despite the simplicity of the reaction, the pathway for the formation of sulfoxides and sulfones has proven to be very complex. Many mechanistic studies have been conducted to elucidate the nature of the reaction intermediates included in the photooxidation of sulfides.[3] Currently, it is accepted that the initially formed intermediate in the oxidation of a sulfide (R_2S) with singlet oxygen is a persulfoxide ($R_2S^+OO^-$).[4]

Photosensitized oxygenation of diorganoselenides to selenoxides was reported by Krief and co-workers,[5] and the process was successfully applied to the reoxidation of osmium catalyst used in the dihydroxylation of olefins.[6]

For the photosensitized oxygenation of organotellurium compounds, Detty and co-workers have shown that the diaryl tellurides and tellurapyrylium dyes act as a chemical quencher of singlet oxygen and afford the corresponding telluroxides or their hydrates.[7] However, there are no synthetic studies on the photosensitized formation of organotellurium oxides from organotellurides and molecular oxygen. In our preliminary communication,[8] we showed that, unlike other diaryl chalcogenides such as Ph_2S and Ph_2Se that are inert to singlet oxygen, the diaryl tellurides react rapidly with singlet oxygen to afford diaryl telluroxides in quantitative yields. Later, the process was applied to the diaryl telluride-catalyzed oxidation of phosphites to phosphates and silanes to silanols.[9] In this paper, we

*To whom correspondence should be addressed. E-mail: moba@tokai-u.jp (M.O.), nishiyam@wing.ncc.u-tokai.ac.jp (K.N.), wataru.ando@aist.go.jp (W.A.).

(1) Schenck, G. O.; Krauch, C. H. *Angew. Chem.* **1962**, *74*, 510.
(2) (a) Ando, W. *Sulfur Rep.* **1981**, *1*, 147–213. (b) Ando, W.; Takada, T. In *Singlet Oxygen*; Frimer, A. A., Ed.; CRC: Boca Raton, FL, 1985; Vol. *3*, pp 1−117. (c) Kim, Y. H. in *Organic Peroxides*; Ando, W., Ed.; John Wiley and Sons Ltd: Chichester, 1992; pp 387−423. (d) Clennan, E. L. In *Advances in Oxygenated Processes*; Baustark, A. L., Ed.; JAI Press: Greenwich, 1995; Vol. *4*, pp 49−80. (e) Clennan, E. L. *Sulfur Rep.* **1996**, *19*, 171–214. (f) Jensen, F. In *Advances in Oxygenated Processes*; Baustark, A. L., Ed.; JAI Press: Greenwich, 1995; Vol. *4*, pp 1−48. (g) Ishiguro, K.; Sawaki, Y. *Bull. Chem. Soc. Jpn.* **2000**, *73*, 535–552.
(3) (a) Foote, C. S.; Peters, J. W. *J. Am. Chem. Soc.* **1971**, *93*, 3795–3796. (b) Liang, J.-J.; Gu, C.-L.; Kacher, M. L.; Foote, C. S. *J. Am. Chem. Soc.* **1983**, *105*, 4717–4721. (c) Nahm, K.; Foote, C. S. *J. Am. Chem. Soc.* **1989**, *111*, 1909–1910. (d) Jensen, F.; Greer, A.; Clennan, E. L. *J. Am. Chem. Soc.* **1998**, *120*, 4439–4449. (e) Clennan, E. L.; Stensaas, K. L.; Rupert, S. D. *Heteroat. Chem.* **1998**, *9*, 51–56. (f) Watanabe, Y.; Kuriki, N.; Ishiguro, K.; Sawaki, Y. *J. Am. Chem. Soc.* **1991**, *113*, 2677–2682. (g) Ishiguro, K.; Hayashi, M.; Sawaki, Y. *J. Am. Chem. Soc.* **1996**, *118*, 7265–7271. (h) Bonesi, S. M.; Fagnoni, M.; Albini, A. *J. Org. Chem.* **2004**, *69*, 928–935. (i) Sofikiti, N.; Rabalakos, C.; Stratakis, M. *Tetrahedron Lett.* **2004**, *45*, 1335–1337. (j) Sofikiti, N.; Stratakis, M. *ARKIVOC* **2003**, 30–35.
(4) Clennan, E. L. *Acc. Chem. Res.* **2001**, *34*, 875–884.
(5) (a) Hevesi, L.; Krief, A. *Angew. Chem.* **1976**, *88*, 413–414. (b) Krief, A.; Lonez, F. *Tetrahedron Lett.* **2002**, *43*, 6255–6257.
(6) (a) Krief, A.; Colaux-Castillo, C. *Pure Appl. Chem.* **2002**, *74*, 107–113. (b) Krief, A.; Colaux-Castillo, C. *Tetrahedron Lett.* **1999**, *40*, 4189–4192. (c) Abatjoglou, A. G.; Bryant, R. D. *Tetrahedron Lett.* **1981**, *22*, 2051–2054.
(7) (a) Serguievski, P.; Detty, M. R. *Organometallics* **1997**, *16*, 4386–4391. (b) Detty, M. R.; Merkel, P. B. *J. Am. Chem. Soc.* **1990**, *112*, 3845–3855.
(8) Oba, M.; Endo, M.; Nishiyama, K.; Ouch, A.; Ando, W. *Chem. Commun.* **2004**, 1672–1673.
(9) (a) Oba, M.; Okada, Y.; Nishiyama, K.; Ando, W. *Org. Lett.* **2009**, *11*, 1879–1881. (b) Okada, Y.; Oba, M.; Arai, A.; Tanaka, K.; Nishiyama, K.; Ando, W. *Inorg. Chem.* **2010**, *49*, 383–385.

Published on Web 10/15/2010

Table 1. Formation of Diaryl Telluroxide **2** and Tellurone **3** by Photosensitized Oxygenation of Diaryl Telluride **1**

$$\underset{\mathbf{1}}{Ar_2Te} \xrightarrow[\text{solvent, 8–15 °C, 1 h}]{h\nu,\ \text{sensitizer, air}} \underset{\mathbf{2}}{Ar_2TeO} + \underset{\mathbf{3}}{Ar_2TeO_2}$$

entry	Ar_2Te (**1**)[a]	solvent (sensitizer[b])	conv. (%)[c]	product ratio[d] (**3**/**2**)	**2** (%)[e]	**3** (%)[e]
1	Ph_2Te (**1a**)	EtOH (RB)	>99	0/100	92	0
2	An_2Te (**1b**)	EtOH (RB)	>99	0/100	99	0
3	Mes_2Te (**1c**)	EtOH (RB)	>99	0/100	99	0
4	Tip_2Te (**1d**)	EtOH (RB)	>99	53/47	*f*	
5	Tip_2Te (**1d**)	CH_2Cl_2 (TPP)	>99	62/38	38	56
6[g]	Tip_2Te (**1d**)	CH_2Cl_2 (TPP)	93	68/32		
7	Tip_2Te (**1d**)[h]	CH_2Cl_2 (TPP)	>99	67/33		
8	Tip_2Te (**1d**)	MeCN (RB)	>99	64/36		
9	Tip_2Te (**1d**)	pyridine (HP)	>99	71/29		
10	MesTipTe (**1e**)	CH_2Cl_2 (TPP)	>99	21/79	79	20
11	Dep_2Te (**1f**)	CH_2Cl_2 (TPP)	>99	25/75	66	18
12	DepTipTe (**1g**)	CH_2Cl_2 (TPP)	>99	37/63	61	28
13	Dip_2Te (**1h**)	CH_2Cl_2 (TPP)	>99	58/42	38	53
14	Dpp_2Te (**1i**)	CH_2Cl_2 (TPP)	no reaction			

[a] An = 4-methoxyphenyl, Mes = 2,4,6-trimethylphenyl, Tip = 2,4,6-triisopropylphenyl, Dep = 2,6-diethylphenyl, Dip = 2,6-diisopropylphenyl, Dpp = 2,6-diphenylphenyl. [b] RB, HP, and TPP denote rose bengal, hematoporphyrin, and tetraphenylporphyrin, respectively. [c] Determined by ^{1}H NMR spectroscopy based on consumed **1**. [d] Determined by ^{1}H NMR spectroscopy. [e] Isolated yield. [f] Not isolated. [g] The reaction was conducted at −65 °C. [h] Concentration at 0.001 M.

describe the photosensitized formation of diaryl tellurones, which are relatively new compounds, in addition to telluroxides. The present study also features bulky diaryl telluroxides as novel and highly efficient trapping agents for the reactive intermediates generated in the oxidation of organochalcogenides with singlet oxygen.

Results and Discussion

Photosensitized Oxygenation of Diaryl Tellurides. Photosensitized oxygenation of diaryl tellurides **1a**−**i** was examined under various reaction conditions, and the results are summarized in Table 1.

When a 0.01 M ethanol solution of Ph_2Te (**1a**) containing rose bengal (RB, 1.00×10^{-4} M) as a photosensitizer in an ice bath (actual reaction temperature increased to 8−15 °C during irradiation) was irradiated under aerobic conditions using a 500 W halogen lamp for 1 h, the ^{1}H NMR spectrum of the reaction mixture showed complete consumption of **1a** and quantitative formation (92% isolated yield) of Ph_2TeO (**2a**) (entry 1). Similar treatment of bis(4-methoxyphenyl) telluride (An_2Te, **1b**) and bis(2,4,6-trimethylphenyl) telluride (Mes_2Te, **1c**) gave the corresponding telluroxides **2b** and **2**c quantitatively (entries 2 and 3). In contrast, the photooxygenation of bis(2,4,6-triisopropylphenyl) telluride (Tip_2Te, **1d**) produced mainly Tip_2TeO_2 (**3d**) along with Tip_2TeO (**2d**) in a ratio of 53:47 (entry 4).[10]

With Tip_2Te as a substrate, reactions in an aprotic solvent, such as dichloromethane, acetonitrile, or pyridine, resulted in an increased ratio of tellurone to telluroxide (entries 5, 8, and 9). This ratio was also increased when the reaction was conducted at low temperature (entry 6) or low concentration (entry 7). Using the same conditions as employed in entry 5, but with a 10-fold concentration of Tip_2Te to facilitate the NMR analysis,

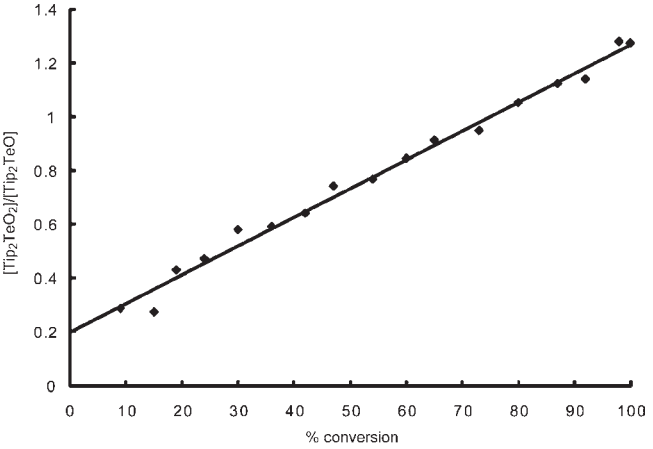

Figure 1. Time course of the photooxygenation of Tip_2Te. The plot of $[Tip_2TeO_2]/[Tip_2TeO]$ versus % conversion (slope = 0.0107, intercept = 0.1994, correlation coefficient, R^2 = 0.9892).

we investigated the time course of the formation of Tip_2TeO and Tip_2TeO_2. The plot of Tip_2TeO_2/Tip_2TeO ratio against the conversion of Tip_2Te yields a linear relationship (correlation coefficient $R^2 = 0.9892$) (Figure 1). This observation indicates that Tip_2TeO may act as a precursor of Tip_2TeO_2. Extrapolation of this ratio to zero conversion, however, does not yield a value of zero, suggesting the existence of an additional pathway for Tip_2TeO_2 formation, in which Tip_2TeO is not involved as a precursor.

To evaluate the effect of bulky substituents on the formation of tellurone, we investigated the photooxygenation of tellurides **1e**−**i** having varying size of aryl substituents, such as Mes, 2,6-diethylphenyl (Dep), 2,6-diisopropylphenyl (Dip), and 2,6-diphenylphenyl (Dpp) groups. As shown in Table 1 (entries 10−13), the proportion of tellurone formation increased from 21% to 58% as the two aryl substituents on the tellurium atom became bulkier. In the case of Dpp_2Te (**1i**), we could not detect any oxidized product, probably because of steric hindrance of the Dpp group (entry 14).

(10) In our preliminary investigations, we did not use an ice bath to maintain the reaction temperature, therefore, the temperature of the reaction mixture rose to 50 °C. At this temperature, the oxidation of Tip_2Te gave Tip_2TeO exclusively.

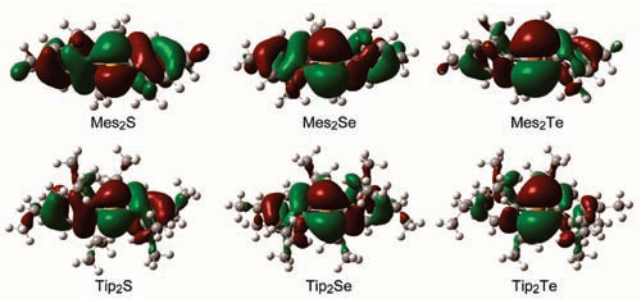

Figure 2. HOMO diagrams for diaryl chalcogenides bearing Mes and Tip groups.

These reactions did not proceed in the dark, without sensitizer, or in the presence of β-carotene (10 mol %), a highly effective singlet oxygen quencher,[11] indicating that the reaction involves singlet oxygen. It is well-known that diaryl chalcogenides such as diphenyl sulfide and selenide are completely inert to singlet oxygen under standard photooxygenation conditions, as employed above.[3a,5b] The enhanced reactivity of diaryl tellurides **1** toward moderately electrophilic singlet oxygen can be attributed to the localized nature of the highest occupied molecular orbitals (HOMOs) at the tellurium atom. Figure 2 shows the HOMOs of Mes_2Te and Tip_2Te, together with those of the sulfides and selenides bearing the same substituents, as calculated by density-functional theory (DFT) methods.[12] The outstanding localization of HOMOs at the chalcogen atom is evident in Mes_2Te and Tip_2Te as compared with the corresponding diaryl sulfides and selenides.

On the basis of the above experimental results, photosensitized oxygenation of Ar_2Te (**1**) to form Ar_2TeO (**2**) and Ar_2TeO_2 (**3**) is assumed to proceed as illustrated in Scheme 1, in a manner similar to the generally accepted mechanism proposed for the oxidation of diorganosulfides with singlet oxygen.[2−4] It begins with the formation of pertelluroxide intermediate **A** by singlet oxygen oxidation of Ar_2Te. If the reaction is performed in alcohol, the intermediate **A** immediately interacts with alcohol to produce hydrogen-bonded pertelluroxide **B** or hydroperoxytellurane **C**, which reacts with the remaining Ar_2Te to give Ar_2TeO exclusively. In the case of Tip_2Te, the alcohol addition might be significantly impeded because of steric hindrance; accordingly, the product distribution becomes similar to that when the reaction is performed in an aprotic solvent described below.

Scheme 1. Plausible Reaction Pathway for the Formation of Ar_2TeO (**2**) and Ar_2TeO_2 (**3**) by the Singlet Oxygen Oxidation of Ar_2Te (**1**)

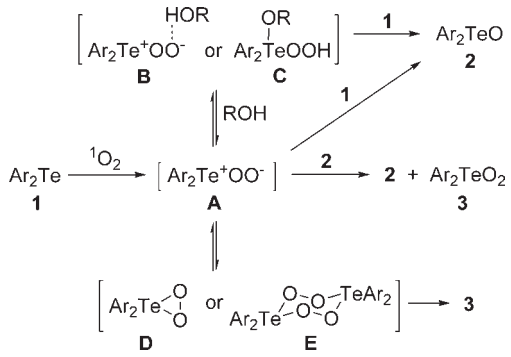

Table 2. Trapping Experiments of the Intermediates Generated in the Photooxygenation of Tip_2Te

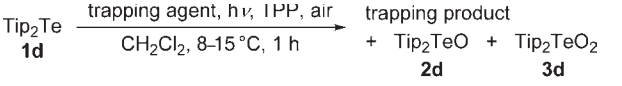

entry	trapping agent	trapping product (%)[a]	**2d** (%)[a]	**3d** (%)[a]
1	Ph_2S	not obtained	41	59
2	Ph_2SO	not obtained	42	58
3	Ph_2Se	not obtained	41	59
4	Ph_2SeO	not obtained	41	59
5	Dep_2TeO	Dep_2TeO_2 (40)	82	18
6	Dip_2TeO	Dip_2TeO_2 (57)	72	28

[a] Determined by ^{1}H NMR spectroscopy.

In an aprotic solvent, the intermediate **A** oxidizes Ar_2Te to form two molecules of Ar_2TeO, which also react with **A** to produce Ar_2TeO_2 along with Ar_2TeO. It follows that the Ar_2TeO_2/Ar_2TeO ratio increases as the reaction proceeds as shown in Figure 1. For consistency with the nonzero intercept in Figure 1, we propose the existence of another pathway for the formation of diaryl tellurones; intramolecular isomerization of dioxatellurirane **D** or homolytic cleavage of the O−O bonds of dimeric intermediate **E**. The increase in the tellurone formation ratio observed in experiments at low temperature or low concentration conditions or with bulky Ar_2Te as a substrate (Table 1) is attributable to the retardation of the intermolecular processes, and thus to the relatively enhanced contribution of the intramolecular process to produce Ar_2TeO_2.

Trapping Experiments. To obtain some insight into the nature of the reaction intermediates produced in the singlet oxygen oxidation of diaryl tellurides, a series of trapping experiments was conducted (Table 2). Various agents to trap the intermediates formed in the reaction of diorganosulfides with singlet oxygen have been reported to date. In this study, we employed Ph_2S,[3b] Ph_2Se,[3i] Ph_2SO,[3b] and Ph_2SeO[3i,j] as trapping agents. In particular, Ph_2SeO is known to be 34 times more reactive than Ph_2SO toward the dimethyl persulfoxide intermediate, Me_2S^+-OO^-, and is recognized as the most efficient trapping agent known so far. Thus, the singlet oxygen oxidation of Tip_2Te was conducted in the presence of an equimolar amount of the above four trapping agents. However, we could not detect any trapping products in the reaction mixture, and the Tip_2TeO_2/Tip_2TeO ratios were essentially

(11) Foote, C. S.; Denny, R. W. *J. Am. Chem. Soc.* **1968**, *90*, 6233–6235.
(12) M., J.; Trucks, G. W.; Schlegel, H. B.; Scuseria, G. E.; Robb, M. A.; Cheeseman, J. R.; Montgomery, J. A., Jr.; Vreven, T.; Kudin, K. N.; Burant, J. C.; Millam, J. M.; Iyengar, S. S.; Tomasi, J.; Barone, V.; Mennucci, B.; Cossi, M.; Scalmani, G.; Rega, N.; Petersson, G. A.; Nakatsuji, H.; Hada, M.; Ehara, M.; Toyota, K.; Fukuda, R.; Hasegawa, J.; Ishida, M.; Nakajima, T.; Honda, Y.; Kitao, O.; Nakai, H.; Klene, M.; Li, X.; Knox, J. E.; Hratchian, H. P.; Cross, J. B.; Bakken, V.; Adamo, C.; Jaramillo, J.; Gomperts, R.; Stratmann, R. E.; Yazyev, O.; Austin, A. J.; Cammi, R.; Pomelli, C.; Ochterski, J. W.; Ayala, P. Y.; Morokuma, K.; Voth, G. A.; Salvador, P.; Dannenberg, J. J.; Zakrzewski, V. G.; Dapprich, S.; Daniels, A. D.; Strain, M. C.; Farkas, O.; Malick, D. K.; Rabuck, A. D.; Raghavachari, K.; Foresman, J. B.; Ortiz, J. V.; Cui, Q.; Baboul, A. G.; Clifford, S.; Cioslowski, J.; Stefanov, B. B.; Liu, G.; Liashenko, A.; Piskorz, P.; Komaromi, I.; Martin, R. L.; Fox, D. J.; Keith, T.; Al-Laham, M. A.; Peng, C. Y.; Nanayakkara, A.; Challacombe, M.; Gill, P. M. W.; Johnson, B.; Chen, W.; Wong, M. W.; Gonzalez, C.; Pople, J. A. *Gaussian 03*, Revision D.02; Gaussian: Wallingford, CT, 2004.

Table 3. Trapping Experiments of Persulfoxide Intermediate $Me_2S^+OO^-$

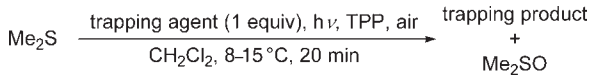

entry	trapping agent	trapping product (%)[a]	Me_2SO (%)[a]
1	Tip_2TeO	Tip_2TeO_2 (>99)	99
2	Dip_2TeO	Dip_2TeO_2 (>99)	99
3	Dep_2TeO	Dep_2TeO_2 (>99)	99
4	Ph_2SO	Ph_2SO_2 (13)[b]	91[b]
5	Ph_2SeO	Ph_2SeO_2 (57)	92

[a] Determined by ^{1}H NMR spectroscopy. [b] Determined by GC.

the same as those observed in the reaction without trapping agents (entries 1−4). These results indicate that the nucleophilicity of the intermediate generated in the photooxygenation of Tip_2Te is relatively low.

We next directed our attention to diaryl telluroxides as trapping agents. When the oxidation of Tip_2Te was performed in the presence of Dep_2TeO, Dep_2TeO_2 was obtained in 40% yield along with Tip_2TeO and Tip_2TeO_2 in a ratio of 82:18 (entry 5). Because Dep_2TeO is completely inert to singlet oxygen as well as both Tip_2TeO and Tip_2TeO_2, the formation of Dep_2TeO_2 can be attributed to the trapping of the nucleophilic pertelluroxide intermediate, $Tip_2Te^+OO^-$ (**A**), by the electrophilic Dep_2TeO. The trapping efficiency of the telluroxide is very high since it trapped the very non-nucleophilic intermediate **A**. Similar treatment of Dip_2TeO also afforded the trapping product, Dip_2TeO_2, in 57% yield (entry 6), suggesting that the bulky telluroxide is more reactive toward the pertelluroxide intermediate **A**. We assume that the observed acceleration of the trapping rate by bulky diaryl telluroxides is also responsible for the preferential formation of the tellurone in the photooxidation of bulky diaryl tellurides.

To evaluate the trapping abilities of the telluroxides relative to conventional trapping agents, trapping experiments of dimethyl persulfoxide, $Me_2S^+OO^-$, were investigated (Table 3). Photosensitized oxygenation of Me_2S was performed in the presence of 1 equiv of Tip_2TeO as a trapping agent. The ^{1}H NMR analysis of the reaction mixture revealed the quantitative formation of Tip_2TeO_2, a trapping product, and Me_2SO (entry 1). Under the reaction conditions employed, Tip_2TeO was completely inert to Me_2SO. Other telluroxides Dip_2TeO and Dep_2TeO also proved to be efficient trapping agents, giving the corresponding tellurone in quantitative yields (entries 2 and 3). For comparison, similar treatment of Ph_2SO[3b] or Ph_2SeO,[3i,j] a well-known trapping agent, was performed; however, the trapping product Ph_2SO_2 or Ph_2SeO_2 was obtained only in 13% or 57% yields, respectively (entries 4 and 5). Apparently, the diaryl telluroxides have higher reactivity toward $Me_2S^+OO^-$ than conventional trapping agents. The trapping rate of $Me_2S^+OO^-$ by Tip_2TeO was measured by direct competition and determined to be k_{rel} = 43 relative to Ph_2SeO (Scheme 2). Tip_2TeO is consequently a new, and most efficient, trapping agent of persulfoxide intermediates.

The highly electrophilic nature of diaryl telluroxides compared with Ph_2SO and Ph_2SeO observed in the trapping experiments is attributable to the localization of lowest unoccupied molecular orbitals (LUMOs) at the

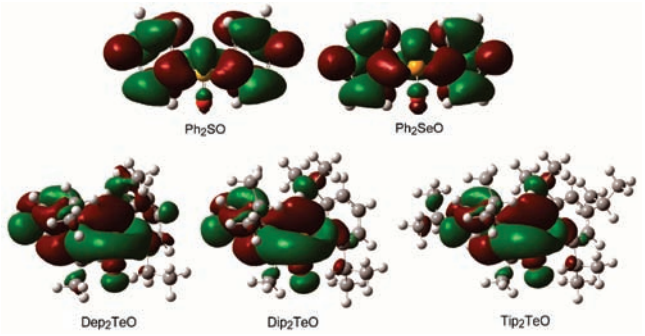

Figure 3. LUMO diagrams for the diaryl telluroxides, Dep_2TeO, Dip_2TeO, and Tip_2TeO, in comparison with Ph_2SO and Ph_2SeO.

Scheme 2. Competitive Trapping of Persulfoxide Intermediate $Me_2S^+OO^-$ by Tip_2TeO with Ph_2SeO

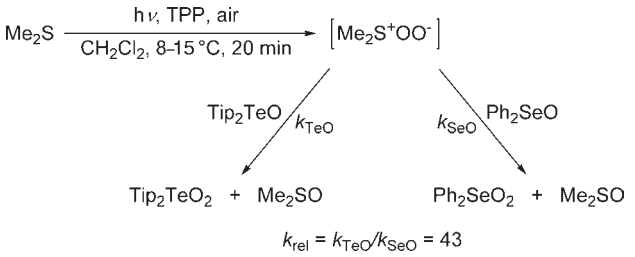

tellurium atom. Figure 3 illustrates the distribution of LUMOs in Dep_2TeO, Dip_2TeO, and Tip_2TeO, as well as Ph_2SO and Ph_2SeO calculated by DFT methods. Apparently greater LUMO localization is observed in Dep_2TeO, Dip_2TeO, and Tip_2TeO than in Ph_2SO and Ph_2SeO.

On the basis of these findings, we investigated the complete conversion of diaryl tellurides to tellurones from a synthetic viewpoint (Table 4). Thus, we performed the photooxygenation of Tip_2Te in the presence of Me_2S (2 equiv), where the persulfoxide $Me_2S^+OO^-$, formed by the reaction of Me_2S and singlet oxygen, was expected to oxidize Tip_2TeO generated in the reaction mixture. The chromatographic purification of the reaction mixture afforded Tip_2TeO_2 in 92% yield. Similar treatment of other tellurides **1e**−**h** also afforded the corresponding tellurones **3e**−**h** in good yields.

Characterization of Diaryl Telluroxides and Tellurones. The structures of diaryl telluroxides and tellurones were confirmed by ^{1}H, ^{13}C, and ^{125}Te NMR, IR, and elemental analysis. The crystal structures of Ph_2TeO and An_2TeO were previously reported by Alcock[13] and Beckmann,[14] respectively. Recently, we succeeded in determining the X-ray crystal structure of Tip_2TeO_2 prepared by $NaIO_4$-oxidation of Tip_2Te, which is the first example of a fully characterized diorganotellurone.[15] In this study, we were able to obtain single crystals of Tip_2TeO and Mes_2TeO, and their structures were unambiguously determined by X-ray crystallographic analysis.

The X-ray structures of Tip_2TeO and Mes_2TeO are shown in Figures 4 and 5, respectively. The molecular

(13) Alcock, N. W.; Harrison, W. D. J. *J. Chem. Soc., Dalton Trans.* **1982**, 709–712.
(14) Beckmann, J.; Dakternieks, D.; Duthie, A.; Ribot, F.; Schürmann, M.; Lewcenko, N. A. *Organometallics* **2003**, *22*, 3257–3261.
(15) Oba, M.; Okada, Y.; Nishiyama, K.; Shimada, S.; Ando, W. *Chem. Commun.* **2008**, 5378–5380.

Table 4. Preparation of Diaryl Tellurone by Co-Photooxygenation of Diaryl Telluride and Me_2S

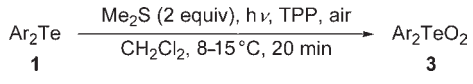

entry	Ar_2Te (**1**)	**3** (%)[a]
1	Tip_2Te (**1d**)	Tip_2TeO_2 (92)
2	MesTipTe (**1e**)	$MesTipTeO_2$ (73)
3	Dep_2Te (**1f**)	Dep_2TeO_2 (69)
4	DepTipTe (**1g**)	$DepTipTeO_2$ (81)
5	Dip_2Te (**1h**)	Dip_2TeO_2 (86)

[a] Isolated yield.

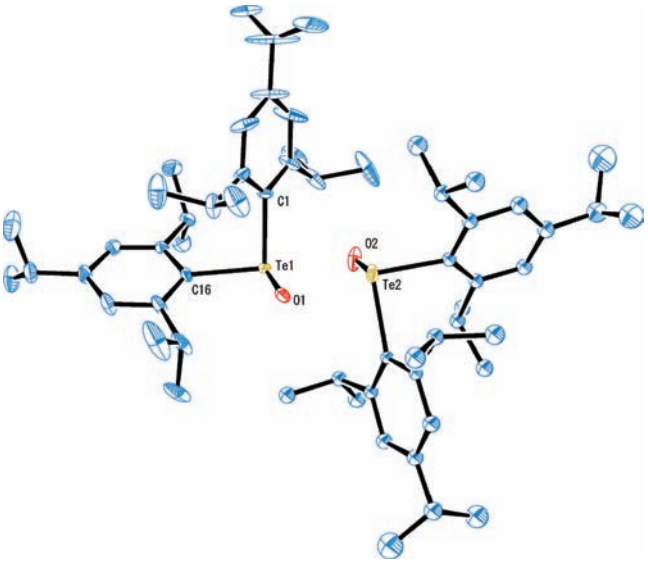

Figure 4. ORTEP diagram of Tip_2TeO (**2d**) with ellipsoids drawn at 30% probability. Hydrogen atoms have been omitted for clarity. Only one orientation of each disordered Tip group attached to the Te2 is displayed. Selected bond distances (Å) and angles (deg): Te1−O1 1.853(5), Te2−O2 1.861(5), Te1−O2 2.536(5), Te2−O1 2.518(4), Te1−C1 2.150(5), Te1−C16 2.191(6), O1−Te1−C1 100.8(2), O1−Te1−C16 101.7(2), C1−Te1−C16 94.7(2).

structure of Tip_2TeO (Figure 4) is essentially the same as those of Ph_2TeO[13] and $(C_6F_5)_2TeO$,[16] adopting a dimeric structure bonded by short intermolecular Te−O interactions (Te1−O2 2.536(5) and Te2−O1 2.518(4) Å). Further Te−O contacts, shorter than the sum of the van der Waals radii (3.58 Å), were not observed.

As shown in Figure 5, the structure of Mes_2TeO also consists of dimers with short secondary Te−O interactions (Te1−O2 2.613(4) and Te2−O1 2.647(4) Å); however, the arrangement of the aromatic rings is different from that of Tip_2TeO. Two Mes groups are located in cis positions with respect to the Te1−O1−Te2−O2 plane, where the CH/π interactions between one *ortho*-methyl proton and the facing aromatic ring are observed. The distances between the protons and the aromatic ring centroids are H11−Ct2 2.940 and H31−Ct1 2.780 Å, which are within the standard range of values.[17] Furthermore,

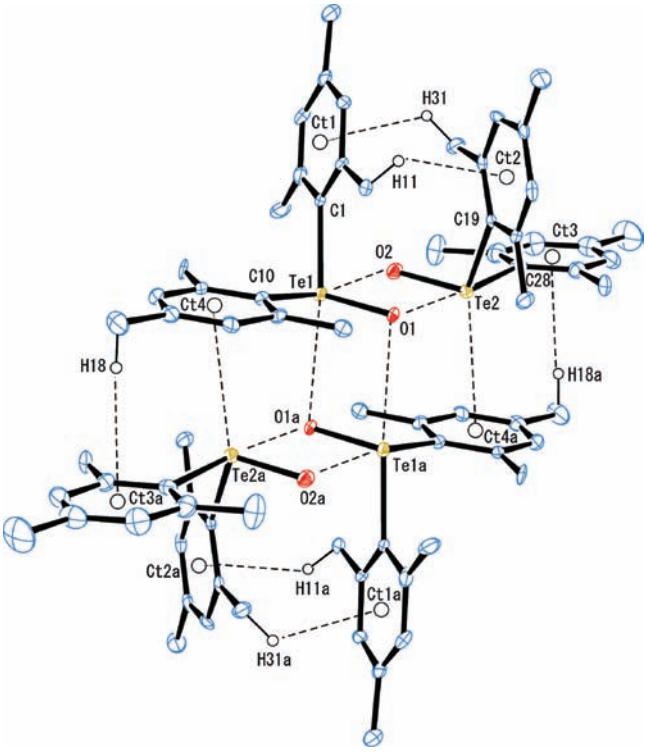

Figure 5. ORTEP diagram of Mes_2TeO (**2c**) with ellipsoids drawn at 30% probability. Hydrogen atoms have been omitted for clarity except for those which participate in intermolecular interactions. Ct1−4 are the centroids of the aromatic rings. Selected bond distances (Å) and angles (deg): Te1−O1 1.855(4), Te2−O2 1.847(4), Te1−O2 2.613(4), Te2−O1 2.647(4), Te1−C1 2.151(7), Te1−C10 2.196(7), Te2−C19 2.131(6), Te2−C28 2.185(7), O1−Te1−C1 105.7(2), O1−Te1−C10 101.5(2), C1−Te1−C10 94.1(2), O2−Te2−C19 104.4(2), O2−Te2−C28 100.9(2), C19−Te2−C28 96.8(2). Symmetry operation used to generate equivalent atoms: a = $-x$, $-y$, $2-z$.

two dimers are linked together by longer secondary Te−O interactions (Te1−O1a 3.040(6) Å, a = $-x$, $-y$, $2-z$) to form a tetrameric structure. A close inspection of the tetramer reveals the existence of Te/π and CH/π interactions between the dimer pairs. The distance between Te2 and Ct4a is 3.324 Å, which is shorter than the average value (ca. 3.8 Å) observed in the crystal structures of organotellurium compounds.[18] It is also assumed that the association of the dimer pairs is further stabilized by the interactions between the *para*-methyl proton of the Mes group and the facing aromatic ring (H18−Ct3a 2.829 Å).

Conclusion

Photosensitized oxidation of diaryl tellurides under aerobic conditions has been investigated. Unlike Ph_2S and Ph_2Se, diaryl tellurides are highly reactive toward weakly electrophilic singlet oxygen to yield diaryl telluroxides and varying amounts of the corresponding tellurone, depending on the substrates and reaction conditions.

The most marked feature of this photooxygenation is the formation of diaryl tellurones in a considerable quantity when a bulky diaryl telluride is employed as a substrate. The trapping experiments of the nucleophilic intermediate, such as $Ar_2Te^+OO^-$ or $Me_2S^+OO^-$, demonstrated that the trapping abilities of the diaryl telluroxides are much higher

(16) (a) Klapötke, T. M.; Krumm, B.; Mayer, P.; Piotrowski, H.; Ruscitti, O. P. Z. *Naturforsch.* **2002**, *57b*, 145–150. (b) Naumann, D.; Tyrra, W.; Hermann, R.; Pantenburg, I.; Wickleder, M. S. Z. *Anorg. Allg. Chem.* **2002**, *628*, 833–842.

(17) Suezawa, H.; Yoshida, T.; Umezawa, Y.; Tsuboyama, S.; Nishio, M. *Eur. J. Inorg. Chem.* **2002**, 3148–3155.

(18) Zukerman-Schpector, J.; Haiduc, I. *CrystEngComm* **2002**, *4*, 178–193.

than those of the conventional trapping agents, and it produces diaryl tellurones very efficiently. In particular, Tip_2TeO is found to be 43 times more reactive than Ph_2SeO. DFT calculations suggest that the highly nucleophilic nature of Ar_2Te and enhanced electrophilicity of Ar_2TeO are attributable to the localization of frontier molecular orbitals, HOMOs and LUMOs, respectively, at the tellurium atom. The time course and other controlled experiments also suggest the possibility of intramolecular pathway for the formation of diaryl tellurones.

Among the diaryl tellurium oxides obtained, molecular structures of Mes_2TeO and Tip_2TeO were determined by X-ray crystallographic analysis.

Experimental Section

NMR Measurements. ^{1}H, ^{13}C, and ^{125}Te NMR spectra were measured on a Varian Mercury plus 400 spectrometer at 400, 100, and 126 MHz, respectively. All chemical shifts are reported as δ values (ppm) relative to residual chloroform (δ_H 7.26), the central peak of deuteriochloroform (δ_C 77.00), and Mes_2Te (δ_{Te} 275). For ^{125}Te NMR, An_2Te (δ_{Te} 667) or Tip_2TeO (δ_{Te} 1319) was used as a secondary external standard.

General Procedure for the Photosensitized Oxygenation of Diaryl Telluride (Table 1). A 10.0 mM solution (50 mL) of diaryl telluride **1** (0.500 mmol) in the presence of an appropriate photosensitizer (1.00×10^{-4} M) was irradiated under aerobic conditions (in an open flask with vigorous stirring) using a 500 W halogen lamp for 1 h. An ice bath was used to maintain the reaction temperature between 8 and 15 °C during irradiation. The progress of the reaction was monitored by TLC. After evaporation of the solvent, the residue was analyzed by ^{1}H NMR spectroscopy to determine the ratio of diaryl telluroxide **2** and tellurone **3**. Diaryl telluroxide **2** and tellurone **3** were isolated using flash column chromatography on silica gel using $CHCl_3$ containing 1% MeOH as the eluent, and the yields are compiled in Table 1. Physical and spectral data of diaryl telluroxides **2a**−**h** and tellurones **3d**−**h** are as follows.

Ph_2TeO (2a).[14] Colorless solid from benzene−hexane, mp 178−181 °C (dec) (lit,[14] mp 182−186 °C (dec)); ^{1}H NMR (400 MHz, $CDCl_3$): δ = 7.37−7.40 (br, 6H), 7.68 ppm (br, 4H); ^{13}C NMR (100 MHz, $CDCl_3$): δ = 129.5, 130.7, 131.0, 138.5 ppm.

An_2TeO (2b).[14] Colorless solid from benzene−hexane, mp 180−183 °C (dec) (lit,[14] mp 185−188 °C (dec)); ^{1}H NMR (400 MHz, $CDCl_3$): δ = 3.81 (s, 6H), 6.95 (d, J = 9 Hz, 4H), 7.60 ppm (d, J = 9 Hz, 4H); ^{13}C NMR (100 MHz, $CDCl_3$): δ = 55.3, 115.2, 128.7, 132.4, 161.8 ppm.

Mes_2TeO (2c).[19] Colorless solid from ethyl acetate, mp 180−182 °C (lit,[19] mp 179−180 °C). ^{1}H NMR (400 MHz, $CDCl_3$): δ = 2.26 (s, 6H), 2.54 (s, 12H), 6.84 (s, 4H) ppm; ^{13}C NMR (100 MHz, $CDCl_3$): δ = 21.2, 21.6, 130.7, 131.1 [s and d (satellite, ^1J (C,Te) = 350 Hz)], 141.1, 143.0 ppm; ^{125}Te NMR (126 MHz, $CDCl_3$, Tip_2TeO): δ = 1268 ppm; IR (KBr): ν = 745 cm^{-1} (Te−O).

Tip_2TeO (2d). Colorless solid from hexane, mp 181−183 °C; ^{1}H NMR (400 MHz, $CDCl_3$): δ = 1.05 (d, J = 7 Hz, 12H), 1.06 (d, J = 7 Hz, 12H), 1.19 (d, J = 7 Hz, 12H), 2.82 (sept, J = 7 Hz, 2H), 3.74 (sept, J = 7 Hz, 4H), 7.01 ppm (s, 4H); ^{13}C NMR (100 MHz, $CDCl_3$): δ = 23.6, 24.1, 24.4, 32.4, 34.0, 123.4, 132.2 [s and d (satellite, ^1J (C,Te) = 346 Hz)], 151.9, 153.0 ppm; ^{125}Te NMR (126 MHz, $CDCl_3$, An_2Te): δ = 1319 ppm; IR (KBr): ν = 740 cm^{-1} (Te−O); elemental analysis calcd (%) for $C_{30}H_{46}OTe$: C 65.48, H 8.43; found: C 65.41, H 8.33.

MesTipTeO (2e).[20] Colorless solid from CH_2Cl_2−hexane, mp 164−165 °C (lit,[20] mp 165−167 °C); ^{1}H NMR (400 MHz, $CDCl_3$): δ = 1.04 (d, J = 7 Hz, 6H), 1.12 (d, J = 7 Hz, 6H), 1.19 (d, J = 7 Hz, 6H), 2.24 (s, 3H), 2.50 (s, 6H), 2.82 (sept, J = 7 Hz, 1H), 3.73 (sept, J = 7 Hz, 2H), 6.80 (s, 2H), 7.00 ppm (s, 2H); ^{13}C NMR (100 MHz, $CDCl_3$): δ = 20.9, 21.4, 23.4, 24.2, 32.5, 34.0, 124.7, 131.2, 136.4 [s and d (satellite, ^1J (C,Te) = 347 Hz)], 137.8 [s and d (satellite, ^1J (C,Te) = 353 Hz)], 141.0, 143.6, 152.5, 154.9 ppm; ^{125}Te NMR (126 MHz, $CDCl_3$, Tip_2TeO): δ = 1320 ppm; IR (KBr): ν = 740 cm^{-1} (Te−O).

Dep_2TeO (2f). Colorless solid from CH_2Cl_2−hexane, mp 151−153 °C; ^{1}H NMR (400 MHz, $CDCl_3$): δ = 1.07 (t, J = 7 Hz, 12H), 2.94 (dq, J = 15 and 7 Hz, 4H), 3.09 (dq, J = 15 and 7 Hz, 4H), 7.09 (d, J = 8 Hz, 4H), 7.30 ppm (t, J = 7 Hz, 2H); ^{13}C NMR (100 MHz, $CDCl_3$): δ = 15.7, 27.6, 127.9, 131.1, 134.7 [s and d (satellite, ^1J (C,Te) = 353 Hz)], 148.8 ppm; ^{125}Te NMR (126 MHz, $CDCl_3$, Tip_2TeO): δ = 1329 ppm; IR (KBr): ν = 750 cm^{-1} (Te−O); elemental analysis calcd (%) for $C_{20}H_{26}OTe$: C 58.59, H 6.39; found: C 58.70, H 6.38.

DepTipTeO (2g). Colorless solid from CH_2Cl_2−hexane, mp 123−124 °C; ^{1}H NMR (400 MHz, $CDCl_3$): δ = 1.07 (d, J = 7 Hz, 6H), 1.07 (t, J = 7 Hz, 6H), 1.12 (d, J = 7 Hz, 6H), 1.20 (d, J = 7 Hz, 6H), 2.84 (sept, J = 7 Hz, 1H), 2.96 (dq, J = 15 and 7 Hz, 2H), 3.08 (dq, J = 15 and 7 Hz, 2H), 3.77 (sept, J = 7 Hz, 2H), 7.03 (s, 2H), 7.09 (d, J = 8 Hz, 2H), 7.28 ppm (t, J = 8 Hz, 1H); ^{13}C NMR (100 MHz, $CDCl_3$): δ = 15.6, 23.7, 24.3, 24.6, 27.4, 32.5, 34.0, 123.4, 127.8, 130.8, 131.8 [s and d (satellite, ^1J (C,Te) = 348 Hz)], 135.3 [s and d (satellite, ^1J (C,Te) = 356 Hz)], 148.5, 152.1, 153.3 ppm; ^{125}Te NMR (126 MHz, $CDCl_3$, Tip_2TeO): δ = 1325 ppm; IR (KBr): ν = 750 cm^{-1} (Te−O); elemental analysis calcd (%) for $C_{25}H_{36}OTe$: C 62.54, H 7.56; found: C 62.62, H 7.91.

Dip_2TeO (2h). Colorless solid from hexane, mp 186−188 °C; ^{1}H NMR (400 MHz, $CDCl_3$): δ = 1.07 (d, J = 7 Hz, 12H), 1.09 (d, J = 7 Hz, 12H), 3.79 (sept, J = 7 Hz, 4H), 7.18 (d, J = 8 Hz, 4H), 7.35 ppm (t, J = 8 Hz, 2H); ^{13}C NMR (100 MHz, $CDCl_3$): δ = 24.3, 24.6, 32.6, 125.5, 131.3, 135.3 [s and d (satellite, ^1J (C, Te) = 347 Hz)], 153.3 ppm; ^{125}Te NMR (126 MHz, $CDCl_3$, Tip_2TeO): δ = 1325 ppm; IR (KBr): ν = 742 cm^{-1} (Te−O); elemental analysis calcd (%) for $C_{24}H_{34}OTe$: C 61.84, H 7.35; found: C 61.75, H 7.31.

Tip_2TeO_2 (3d).[15] Colorless solid from hexane, mp 108−110 °C (lit,[15] mp 108−110 °C). ^{1}H NMR (400 MHz, $CDCl_3$): δ = 1.12 (d, J = 7 Hz, 24H), 1.21 (d, J = 7 Hz, 12H), 2.88 (sept, J = 7 Hz, 2H), 4.09 (sept, J = 7 Hz, 4H), 7.14 ppm (s, 4H); ^{13}C NMR (100 MHz, $CDCl_3$): δ = 23.6, 24.3, 32.7, 34.3, 124.8, 137.9 [s and d (satellite, ^1J (C,Te) = 81 Hz)], 152.2, 154.8 ppm; ^{125}Te NMR (126 MHz, $CDCl_3$, Tip_2TeO): δ = 1331 ppm; IR (KBr): ν = 800, 825 cm^{-1} (Te−O).

$MesTipTeO_2$ (3e). Colorless solid from acetonitrile, mp 126−128 °C; ^{1}H NMR (400 MHz, $CDCl_3$): δ = 1.14 (d, J = 7 Hz, 12H), 1.22 (d, J = 7 Hz, 6H), 2.28 (s, 3H), 2.69 (s, 6H), 2.88 (sept, J = 7 Hz, 1H), 4.06 (sept, J = 7 Hz, 2H), 6.95 (s, 2H), 7.15 ppm (s, 2H); ^{13}C NMR (100 MHz, $CDCl_3$): δ = 20.9, 21.3, 23.4, 24.2, 32.5, 34.0, 124.7, 131.2, 136.4 [s and d (satellite, ^1J (C,Te) = 90 Hz)], 137.9 [s and d (satellite, ^1J (C,Te) = 95 Hz)], 140.9, 143.6, 152.5, 154.9 ppm; ^{125}Te NMR (126 MHz, $CDCl_3$, Tip_2TeO): δ = 1333; elemental analysis calcd (%) for $C_{24}H_{34}O_2Te \cdot H_2O$: C 57.64, H 7.26; found: C 57.95, H 7.39.

Dep_2TeO_2 (3f). Colorless solid from acetonitrile, mp 134−138 °C; ^{1}H NMR (400 MHz, $CDCl_3$): δ = 1.18 (t, J = 7 Hz, 12H), 3.22 (q, J = 7 Hz, 8H), 7.26 (d, J = 8 Hz, 4H), 7.49 ppm (t, J = 8 Hz, 2H); ^{13}C NMR (100 MHz, $CDCl_3$): δ = 15.9, 28.0, 129.4, 133.6, 140.6 [s and d (satellite, ^1J (C,Te) = 99 Hz)], 147.8 ppm; ^{125}Te NMR (126 MHz, $CDCl_3$, Tip_2TeO): δ = 1332 ppm; elemental analysis calcd (%) for $C_{20}H_{26}O_2Te \cdot H_2O$: C 56.42, H 7.58; found: C 56.68, H 7.45.

$DepTipTeO_2$ (3g). Colorless solid from hexane, mp 137−140 °C; ^{1}H NMR (400 MHz, $CDCl_3$): δ = 1.16 (t, J = 7 Hz, 6H),

(19) Akiba, M.; Lakshmikantham, M. V.; Jen, K.-Y.; Cava, M. P. *J. Org. Chem.* **1984**, *49*, 4819–4821.
(20) Taka, H.; Yamazaki, Y.; Shimizu, T.; Kamigata, N. *J. Org. Chem.* **2000**, *65*, 2127–2133.

1.16 (d, J = 7 Hz, 12H), 1.24 (d, J = 7 Hz, 6H), 2.91 (sep, J = 7 Hz, 1H), 3.23 (q, J = 7 Hz, 4H), 4.11 (sep, J = 7 Hz, 2H), 7.17 (s, 2H), 7.25 (d, J = 8 Hz, 2H), 7.46 ppm (t, J = 8 Hz, 1H); ^{13}C NMR (100 MHz, $CDCl_3$): δ = 15.7, 23.5, 24.3, 27.8, 32.8, 34.2, 125.0, 129.2, 133.3, 137.3 [s and d (satellite, ^1J(C,Te) = 89 Hz)], 141.1 [s and d (satellite, ^1J(C,Te) = 95 Hz)], 147.4, 152.5, 155.1 ppm; ^{125}Te NMR (126 MHz, $CDCl_3$, Tip_2TeO): δ = 1332 ppm; elemental analysis calcd (%) for $C_{25}H_{36}O_2Te \cdot 2H_2O$: C 56.42, H 7.58; found: C 56.68, H 7.45.

Dip_2TeO_2 (3h). Colorless solid from hexane, mp 194−195 °C; ^{1}H NMR (400 MHz, $CDCl_3$): δ = 1.13 (d, J = 7 Hz, 24H), 4.13 (sept, J = 7 Hz, 4H), 7.32 (d, J = 8 Hz, 4H), 7.51 ppm (t, J = 8 Hz, 2H); ^{13}C NMR (100 MHz, $CDCl_3$): δ = 24.3, 32.8, 126.9, 133.6, 140.8 [s and d (satellite, ^1J(C,Te) = 85 Hz)], 152.3 ppm; ^{125}Te NMR (126 MHz, $CDCl_3$, Tip_2TeO): δ = 1331 ppm; IR (KBr): ν = 800, 822 cm^{-1} (Te−O); elemental analysis calcd (%) for $C_{24}H_{34}O_2Te$: C 59.79, H 7.11; found: C 59.55, H 7.23.

General Procedure for the Photosensitized Co-Oxygenation of Tip_2Te (1d) and Various Trapping Agents (Table 2). A 10.0 mM CH_2Cl_2 solution (50 mL) of **1d** (267 mg, 0.500 mmol) containing 1.00 equiv of a trapping agent was irradiated in the presence of tetraphenylporphyrin (1.00×10^{-4} M) as a photosensitizer. After 1 h, the solvent was evaporated, and the residue was analyzed by ^{1}H NMR spectroscopy to determine the product distribution. The yields of the trapping product as well as **2d** and **3d** are compiled in Table 2.

General Procedure for the Trapping Experiments of the Persulfoxide Intermediate by Ar_2TeO, Ph_2SO, or Ph_2SeO (Table 3). To a 10.0 mM CH_2Cl_2 solution (50 mL) of trapping agent (0.500 mmol) containing tetraphenylporphyrin (1.00×10^{-4} M) as a photosensitizer was added a 1.00 M CH_2Cl_2 solution of Me_2S (0.500 mL, 1.00 mmol), and the solution was irradiated for 20 min. After evaporation of the solvent, the residue was analyzed by ^{1}H NMR spectroscopy to determine the product distribution. The yields of the trapping product, such as Ar_2TeO_2, Ph_2SO_2, or Ph_2SeO_2, and Me_2SO are compiled in Table 3.

Competitive Trapping of the Persulfoxide Intermediate by Tip_2TeO (2d) and Ph_2SeO (Scheme 2). To a solution of **2d** (57.4 mg, 0.104 mmol) and Ph_2SeO (249.3 mg, 1.00 mmol) in CH_2Cl_2 (50 mL) containing tetraphenylporphyrin (1.00×10^{-4} M) as a photosensitizer was added a 1.00 M CH_2Cl_2 solution of Me_2S (50.0 μL, 50.0 μmol) and the solution was irradiated for 20 min. After evaporation of the solvent, the residue was analyzed by ^{1}H NMR spectroscopy to determine the ratio of **3d** and Ph_2SeO_2. Three runs were averaged and the trapping rate of $Me_2S^+OO^-$ by **2d** relative to Ph_2SeO was determined to be k_{rel} = 43. Under the conditions employed, Ph_2SeO_2 and Tip_2TeO_2 were completely inert to Tip_2TeO and Ph_2SeO, respectively.

General Procedure for the Photosensitized Co-Oxygenation of Ar_2Te with Me_2S (Table 4). A 10.0 mM CH_2Cl_2 solution (50 mL) of Ar_2Te (0.500 mmol) and 2 equiv of Me_2S was irradiated in the presence of tetraphenylporphyrin (1.00×10^{-4} M) as a photosensitizer for 20 min. After evaporation of the solvent, the residue was chromatographed on silica gel using $CHCl_3$ as the eluent. The isolated yields of the Ar_2TeO_2 are listed in Table 4.

Theoretical Calculations. All calculations were performed using the Gaussian 03 program package.[12] The geometries were optimized with the density functional theory at the B3PW91 level. The LANL2DZdp basis set was used for Se and Te, while the 6-31G(d,p) basis set was used for C, H, and O. Stationary points were confirmed to be minima by vibrational frequency calculations that gave no imaginary frequencies.

Crystal Data for Mes_2TeO (2c). $C_{18}H_{22}OTe$, M = 381.97, crystal dimensions 0.20 × 0.17 × 0.06 cm^3, orthorhombic, a = 16.8808(12), b = 29.017(2), c = 13.8314(10) Å, V = 6775.2(8) Å^3, T = 153(2) K, space group $Pccn$ (#56), Z = 16, ρ_{calcd} = 1.498 g cm^{-3}, μ(Mo Kα) = 1.751 mm^{-1}, 38271 reflections measured, 7698 independent reflections (R_{int} = 0.070). The final R_1 values were 0.0495 ($I > 2\sigma(I)$). The final $wR(F^2)$ values were 0.1190 (all data). The goodness of fit on F^2 was 1.063. CCDC-773378 contains the supplementary crystallographic data for this compound. These data can be obtained free of charge from The Cambridge Crystallographic Data Centre via www.ccdc.cam.ac.uk/data_request/cif.

Crystal Data for Tip_2TeO (2d). $C_{30}H_{46}OTe$, M = 550.29, crystal dimensions 0.16 × 0.14 × 0.10 cm^3, monoclinic, a = 9.1860(5), b = 22.2220(13), c = 28.6662(17) Å, β = 96.2280(10)°, V = 5817.1(6) Å^3, T = 153(2) K, space group $C1c1$ (#1), Z = 8, ρ_{calcd} = 1.257 gcm^{-3}, μ(Mo Kα) = 1.041 mm^{-1}, 17355 reflections measured, 11719 independent reflections (R_{int} = 0.027). The final R_1 values were 0.0508 ($I > 2\sigma(I)$). The final $wR(F^2)$ values were 0.1264 (all data). The goodness of fit on F^2 was 1.025. CCDC-773379 contains the supplementary crystallographic data for this compound. These data can be obtained free of charge from The Cambridge Crystallographic Data Centre via www.ccdc.cam.ac.uk/data_request/cif.

Acknowledgment. Financial support from Tokai University is gratefully acknowledged by M.O.

Supporting Information Available: General experimental information; procedures for the preparation of tellurides **1**, Ph_2SeO, and Ph_2SeO_2; copies of ^{1}H, ^{13}C, and ^{125}Te NMR and IR spectra for selected compounds; and X-ray crystallographic data for **2c** and **2d** in CIF format. This material is available free of charge via the Internet at http://pubs.acs.org.